A New Linear Quadratic Optimal Controller for the 34-Meter High Efficiency Antenna Position Loop

J. A. Nickerson

Ground Antenna and Facilities Engineering Section

This article explores the design of a new position loop controller for the 34-m High Efficiency Deep Space antennas using linear quadratic (LQ) optimal control techniques. The LQ optimal control theory is reviewed, and model development and verification are discussed. Families of optimal gain vectors were generated by varying weight parameters. Performance specifications were used to select a final gain vector. Estimator dynamics were selected and the corresponding gain vectors were computed. Final estimator selection was based on position, commanded rate, and estimator error responses.

I. Introduction

This article investigates the application of linear quadratic (LQ) optimal control technique for designing a new position loop tracking controller for the 34-m high efficiency ground based antenna. Most antenna controllers consist of an analog rate loop and a position loop closed with a computer. Two different types of control algorithms typically used for antenna position control are proportional-integral (PI) controllers and state feedback controllers.

Proportional-integral control is accomplished by applying gains to position error and the integral of position error. The summed result is used as a commanded rate for the rate loop. Zero steady state error to a ramp input (a type II system) is realized with a PI controller. This type of controller, however, can not arbitrarily specify the eigenvalues of the closed position loop.

A more sophisticated controller which can arbitrarily specify the eigenvalues of the closed position loop is state feedback. This requires representing the control system as a set of first order differential state equations and multiplying each state by a gain. The summed results are used as a commanded rate for the rate loop. State feedback is more difficult to implement than PI control because PI controllers need only have knowledge of the position error while state feedback requires knowledge of all states. Unfortunately, many states are inaccessible to measure or state measurement is cost prohibitive. The use of a dynamic estimator, which estimates the value of each state based on a plant model and measurable states, solves this problem. The gains for implemented state controllers are often calculated based on designer selected eigenvalues.

The new approach explored in this article uses linear quadratic (LQ) optimal control to calculate families of gain vectors. Final gain selection is based on meeting desired performance criteria. After the control-gain design is completed, another design procedure is required for the estimator. Several estimator gains are designed and simulated with the

final control gain. Estimator gain selection is based on system performance specifications, minimal estimator error, and insensitivity to encoder and digital to analog (D/A) quantization.

II. Theory

The plant can be linearly modeled by a set of first order differential equations of the form:

$$\dot{x} = Ax + Bu \; ; x(0) = x_0$$
$$y = Cx \tag{1}$$

where x is an $n \times 1$ state column vector; u is a $1 \times m$ input row vector; y is a $1 \times m$ output column vector; A, B, and C are coefficient matrices of appropriate dimensions. A commonly used control design is state variable feedback:

$$u = -Kx \tag{2}$$

where K is a feedback gain vector, not necessarily producing an optimum controller. Substituting Eq. (2) into Eq. (1) yields:

$$\dot{x} = Ax - BKx$$
$$\dot{x} = (A - BK)x \tag{3}$$

Equation (3) suggests that plant dynamics are modified by the feedback gain vector K. State feedback is attractive because the closed loop eigenvalues of the system are arbitrarily specified by the proper selection of the feedback vector K. Numerical procedures exist which calculate K for a desired set of eigenvalues (see [4]). Although a designer can iterate a pole selection until the closed loop system meets performance criteria, there are no guarantees that the design is optimal.

The LQ optimal control technique for a linear system uses a quadratic performance index as an optimality criterion. Given the system description in Eq. (1) the quadratic performance index J is of the form:

$$J = \int_0^\infty (x^T Q x + \rho u^T R u)\, dt \tag{4}$$

where Q is a positive semi-definite matrix, R is a positive definite matrix, and ρ is a positive non-zero scalar. The first term penalizes transient deviation of the state from the origin. The second term penalizes the amount of control effort used to control the states. Terms Q, R, and ρ are weighting terms

which adjust penalties for transient deviation and control effort. The solution for the standard LQ problem is given elsewhere [1], [3], [4]; therefore, only the results are summarized below. The optimal steady state solution yields the control law:

$$u = -Kx \tag{5}$$

where

$$K = R^{-1}B^T P \tag{6}$$

P is a symmetric positive semi-definite solution to the Riccatti equation in matrix form:

$$A^T P + PA + Q - PBR^{-1}B^T P = 0 \tag{7}$$

The steady state solution exists if the following conditions are met:

(1) the controlled plant is controllable or can be stabilized,

(2) the final time is $t = \infty$, and

(3) $(A, Q^{1/2})$ is observable.

Numerical procedures are used to solve the Riccatti equation and calculate K knowing the system and weighting matrices (see [4]).

The LQ optimal design technique for state feedback control guarantees an infinite gain margin and a greater than 60 degree phase margin for continuous (analog) systems. The final implementation of this controller is a time-discretized (digital) form. Stability for the time-discretized case is degraded from the continuous case because of finite sampling time. Tomizuka [1] investigated gain and phase margin for the discretized controller using:

$$\text{Gain Margin} > \frac{1}{1 - \sqrt{\dfrac{F}{F + \Gamma^T H \Gamma}}}$$
$$\text{Phase Margin} > 2 \sin^{-1} \left\{ \frac{1}{2} \sqrt{\frac{F}{F + \Gamma^T H \Gamma}} \right\} \tag{8}$$

where H is the solution to the discrete version of the Riccati equation, F is the product $R\rho$, and Γ is the discretized version of B. A complete discussion of the discretized case may be found in [1].

Implementation of state feedback requires knowledge of the entire state vector. When states are unmeasured they must be estimated. A closed-loop estimator is based on a plant

model and the weighted difference between the estimated and actual output. Figure 1 describes state feedback implementation using an estimator. The estimator equation takes the form of:

$$\dot{\hat{x}} = A\hat{x} + Bu + L(y - C\hat{x}) \; ; \hat{x}(0) = \hat{x}_0 \qquad (9)$$

where L is the estimator error gain vector and x represents the estimated state vector. Rewriting Eq. (9) yields:

$$\dot{\hat{x}} = (A - LC)\hat{x} + Bu + Ly \qquad (10)$$

Subtracting Eq. (10) from Eq. (1) produces the equation describing the estimator error dynamics.

$$\dot{e} = (A - LC)e \qquad e = (x - \hat{x}) \qquad (11)$$

Equation (11) is similar to Eq. (3). The error dynamics can be shown to depend on the selection of L. Therefore, error dynamics are selected and a pole placement algorithm is used to calculate the estimator gain vector.

The closed-loop system dynamics depend on the combined eigenvalues of the controller and the estimator. However, the controller design is independent of the estimator design because estimator gains do not alter controller dynamics and controller gains do not alter estimator dynamics.

III. Modeling

Before LQ design techniques were applied, a plant model was developed. Figure 2 presents the linear model of the rate loop for the 34-m high efficiency AZ-EL antenna. Simplifying the model by eliminating fast dynamics (i.e., using large negative eigenvalues) and normalizing yielded the transfer function:

$$G(s) = \frac{Y(s)}{U(s)} = \frac{491.2\,(0.94s + 1)}{s^2 + 46.18s + 491.2} \qquad (12)$$

where $U(s)$ is the input rate in degrees per second and $Y(s)$ is output rate in degrees per second. The simplified model in Eq. (12) represents a rigid antenna without structural dynamics.

Verification of the simple rate loop model of Eq. (12) was accomplished by using an HP dynamic signal analyzer, model 3562A, to measure the swept-sinusoid frequency response of the elevation rate loop at DSS (Deep Space Station) 15. Figures 3 and 4 present the measured gain and phase responses, respectively. The gain and phase responses were curve fit to produce a transfer function model for comparison with the simplified theoretical model. Curve fit results are shown in Figs. 5 and 6. Goodness-of-fit is shown by com-

paring measured and curve fit data in Figs. 3 and 5 for gain response and Figs. 4 and 6 for phase response. The transfer function description of the curve fit is:

$$G(s) = \frac{472.1\,(0.12s + 1)\,(s^2 + 0.667s + 188.0)}{(s^2 + 55.4s + 472.1)\,(s^2 + 1.11s + 187.3)}$$

$$\times \frac{(s^2 + 0.534 + 440.2)}{(s^2 + 0.610s + 422.6)} \qquad (13)$$

Eliminating polynomials due to structural resonances in Eq. (13) yields:

$$G(s) = \frac{472.1\,(0.12s + 1)}{s^2 + 55.4s + 472.1} \qquad (14)$$

Comparing Eq. (12) with Eq. (14) suggests the model simplification of Eq. (12) was reasonable in the frequency range between 0.1 to 10 Hz.

Optimal control techniques require a state representation of the plant model. Transforming Eq. (12) into a diagonal canonical set of state equations of the form in Eq. (1) yielded:

$$\dot{x} = \begin{bmatrix} -29.56 & 0 \\ 0 & -16.62 \end{bmatrix} x + \begin{bmatrix} 8.217 \\ 4.62 \end{bmatrix} u$$

$$y = [8.217, -4.619]\, x \qquad (15)$$

where u is input rate and y is output rate. The state equations were then augmented to include position and integral of position states. Augmenting required increasing the dimension of A from 2 × 2 to 4 × 4, the dimension of B from 2 × 1 to 4 × 1, and the dimension of C from 1 × 2 to 1 × 4.

$$\begin{Bmatrix} x_1 \\ x_2 \\ x_3 \\ x_4 \end{Bmatrix} = \begin{bmatrix} 0 & 1 & 0 & 0 \\ 0 & 0 & 8.217 & -4.619 \\ 0 & 0 & -29.56 & 0 \\ 0 & 0 & 0 & -16.62 \end{bmatrix} \begin{Bmatrix} x_1 \\ x_2 \\ x_3 \\ x_4 \end{Bmatrix}$$

$$+ \begin{bmatrix} 0 \\ 0 \\ 8.217 \\ 4.619 \end{bmatrix} u \qquad (16)$$

The new states are integral of position, x_1, and position, x_2, the input u is a rate command. The augmented state equations with state feedback produce a type II position controller. A diagonal canonical form of the state equation was used to reduce computations for implementation and to ensure reasonable matrix numerical conditioning.

Equation (16) describes a regulator. Once a gain vector, K, was calculated, implementation required altering the regulator equations to track reference inputs. The position state became position error and integral of position became integral of position error.

IV. LQ Controller Design

The LQ design approach depends on weighting matrix selection. Relative magnitude of weighting determines the optimal result. Coefficient selection, however, is not intuitive and guidelines are helpful. Bryson and Ho [3] suggest the simple rule:

$$Q = \text{diag} \frac{1}{\|x_{i_{max}}\|} \qquad (17)$$

where $x_{i_{max}}$'s are the maximum values allowed for the ith state. Off diagonal terms are zero. A unit step response suggests $x_{11} = 1$ (position error). Weighting position error and rate loop dynamics equally yielded:

$$Q_{22} = Q_{33} = Q_{44} = 1 \qquad (18)$$

Assuming a 0.5 second rise time, $Q_{11} = 4.0$. Q_{11} will be less than 4.0 for longer rise times. R and ρ are scalars for a single input single output (SISO) system. Thus, R was set equal to 1 and only ρ was parameterized to vary control effort penalties. A continuous LQ formulation was used to calculate the control gain vector K. The sampling time for the controller was selected as 50 Hz because of the high rate loop bandwidth. The fast sampling time allowed computed continuous gain vectors to be used with the discretized system.

The optimal control gains were calculated for different Q_{11} and ρ combinations. Several families of gain vectors were computed for each Q_{11} by varying ρ. Table 1 lists the results of several control gain computations. The table contains calculated gains and resulting closed-loop eigenvalues for each $Q_{11} - \rho$ combination.

Each control gain design iteration was simulated using the model in Eq. (16). Figures 7, 8, 9, and 10 represent simulated 50 millidegree step responses for several control gain vectors. Each figure shows a family of curves based on gains resulting

from a constant Q matrix but with different ρ values. The figures show that smaller values of ρ, which reduce control effort penalties, produced a greater control effort and thereby reduced system overshoot and settling time. Larger values of Q_{11} increased step response overshoot and reduced settling time. System overshoot, as a function of Q_{11} is obtained from the corresponding closed-loop eigenvalues in Table 1. Increasing Q_{11} reduced system damping.

Performance specifications for this LQ controller require: (1) the closed position loop response have less than 40 percent overshoot for small position steps and (2) a minimum position loop bandwidth of 0.25 Hz. The step responses in Figs. 7, 8, 9, and 10 have overshoots less than 20 percent, and hence are acceptable. Bandwidth is limited by the presence of structural resonances. Rate loop structural resonances are as low as 2.3 Hz. The position loop bandwidth must be at least an octave below the first structural resonance; otherwise the position loop may excite the structural resonances. Therefore, the position loop bandwidth should remain below 0.43 Hz. Figures 11, 12, 13, and 14 are closed-loop frequency responses using gain vectors obtained from Table 1 which best satisfy the 0.43 Hz position loop bandwidth goal. The bandwidths range from 0.39 to 0.43 Hz. The four Q and ρ combinations which satisfy the bandwidth criterion are:

K_A :	$Q_{11} = 4$	$\rho = 1.5$	bw = 0.43 Hz
K_B :	$Q_{11} = 2$	$\rho = 1.0$	bw = 0.41 Hz
K_C :	$Q_{11} = 1$	$\rho = 0.6$	bw = 0.40 Hz
K_D :	$Q_{11} = 0.5$	$\rho = 0.4$	bw = 0.39 Hz

Final gain vector selection was based on a performance index. The integral of time multiplied by absolute error (ITAE) index, I, was chosen because it places emphasis on errors occurring later in time [2]. The general form of the performance index is:

$$I = \int_0^T t |e(t)| dt \qquad (19)$$

where T is the study period, t represents time, and $e(t)$ is the position error. The ITAE index was calculated for the four possible gain vectors with T equal to 5 seconds. K_A produced the lowest index value relative to K_B, K_C, and K_D and was selected as the final control gain.

Consequently, stability margins were calculated for control gain K_A using Eq. (8). The steady state discrete Riccati equation solution was calculated based on gain vector K_A. The gain

margin for the discretized system is 14.6 dB with a phase margin of 48 degrees. Gain and phase margin values indicate K_A is a robust controller design for the discrete system.

V. Estimator Design

The estimator design procedure consisted of selecting estimator dynamics and computing the estimator gain vector. The integral-of-position error is easily obtained in real time by numerical integration. Therefore, a third order estimator was designed. A discretized version of the third order plant model for 50 Hz implementation was used to calculate estimator gains. Equation (20) is the discretized third order model.

$$x(k+1) = \begin{bmatrix} 1 & 0.1268 & -0.7922 \\ 0 & 0.5437 & 0 \\ 0 & 0 & 0.7150 \end{bmatrix} x(k) + \begin{bmatrix} 0.01167 \\ 0.0979 \\ 0.0679 \end{bmatrix} u(k)$$

(20)

where k represents discrete time. Eight sets of dynamic parameters were selected and an estimator gain vector calculated for each set. Table 2 presents the pole locations and calculated gain vectors for each design iteration. Estimator and controller gains were simulated using the curve fit rate loop with structural dynamics as the actual plant. Plant output rate was integrated to calculate position. Encoder and D/A quantizing effects were also simulated. Estimator performance was based on position response, command rate, and estimator error. The position response should display the same performance as discussed under controller design. Command rate is equivalent to the output of the D/A converter. Local monotonicity of the command rate response is desirable to eliminate the position controller exciting structual resonances. (Local monotonicity suggests that within a limited time frame the command rate is either steadily increasing or steadily decreasing.) Therefore, the command rate should be a smooth function. Estimator error (actual position minus estimated position) should be much less than one least significant bit of the encoder (0.0003433 degrees) for the 20-bit encoder. Satisfying this error criterion will maintain precision pointing and reduce possible limit cycling due to the accumulation of large estimator errors.

The results of the position, commanded rate, and estimator error responses were used to judge estimator dynamics. Figures 15, 16, 17, and 18 show position and commanded rate response simulations for estimators 2, 3, 4, and 7, respectively. The position response curves for all estimators are similar. Selecting the "best" estimator based on position response is difficult. Commanded rate responses were next analyzed.

Estimators 2, 4, and 7 produced commanded rate responses which do not have "good" local monotonicity; the commanded rate in Figs. 19, 21, and 22 oscillated between D/A quantization levels. Estimator 3 (Fig. 20) had between 60 percent and 84 percent fewer oscillations than the other estimators and produced the smoothest commanded rate response.

Local monotonicity is a function of estimator dynamics. Each new position quantization level causes a step in estimator error. Estimators respond to steps in error as a function of their eigenvalues. Estimators 2 and 4 have eigenvalues which cause overshoot in the estimator error response. The overshooting increased the estimator error and caused the loss of local monotonicity. On the other hand, estimator 7 has heavily damped eigenvalues. Estimator 7's error response could not respond quickly to changing position. Thus, sluggish response of estimator 7 reduced local monotonicity. Estimator 3 has the best response; the error response has no overshoot to changes in position yet its dynamics were fast. The fast, critically damped estimator response also has the smallest overall error. The selected control design uses the control gain vector K_A and the estimator gain vector L_3.

VI. Summary

Linear quadratic (LQ) optimal control techniques were applied to developing a new type II, state feedback, antenna position controller. A simplified experimental transfer function model was developed and verified by curve frequency response data. The model was mapped into a diagonal canonical set of state equations which were augmented to include position and integral-of-position states. Weighting matrices were selected and families of optimal gains were calculated based on the augmented model. The closed-loop system was simulated with each gain vector and the "best" gain was selected based on meeting given performance specifications. The integral-of-position state was eliminated and the third order model was used to design a new state estimator. Estimator dynamics were selected and estimator gain vectors calculated. The selected control gain vector was simulated with each estimator gain vector using a high order plant model with model mismatch, structural resonances, and quantization affects. An estimator gain vector was selected which minimized quantizing effects and estimator error.

This article described LQ optimal controller and estimator design techniques for an antenna position controller. Final design selection was based on satisfying performance specifications. The performance specifications, however, are not necessarily optimal. Investigations are needed which will determine the optimal performance requirements for this system. Once new performance criteria are determined, the LQ optimal controller and the estimator can be redesigned.

Acknowledgements

References

[1]   M. Tomizuka, ME 232 Advanced Control Systems I, Class Notes, Univ. of Berkeley, CA, Dept. of Mechanical Engineering, 1984.

[2]   R. C. Dorf, *Modern Control Systems*. 3rd ed., Reading, Mass.: Addision-Wesley Publishing Co., 1983.

[3]   A. E. Bryson, Jr. and Y. Ho, *Applied Optimal Control*. Waltham, Mass.: Blaisdell Publishing Co., 1969.

[4]   G. F. Franklin and J. D. Powell, *Digital Control of Dynamic Systems*. Reading, Mass.: Addison-Wesley Publishing Co., 1980.

Table 1. Calculated control gain vectors and eigenvalues

Q_{11}	ρ	K_1	K_2	K_3	K_4	Eigenvalues (rad/s)
4	4	1.000	1.513	0.442	−0.6694	
	2	1.414	1.854	0.563	−0.4246	
	1.5	1.633	2.024	0.628	−0.4472	$-0.964 \pm j\,0.789, -17.052, -30.298$
	1	2.000	2.300	0.740	−0.4772	
	0.5	2.828	2.903	1.009	−0.5175	
2	2	1.000	1.605	0.498	−0.3613	
	1	1.414	2.008	0.665	−0.4037	$-0.935 \pm j\,0.663, -17.243, -30.672$
	0.9	1.491	2.081	0.697	−0.4091	$-0.962 \pm j\,0.670, -17.304, -30.797$
	0.5	2.000	2.559	0.923	−0.4310	
1	1	1.000	1.773	0.605	0.3435	
	0.7	1.195	2.015	0.719	−0.3555	$-0.912 \pm j\,0.497, -17.468, -31.157$
	0.6	1.291	2.133	0.777	−0.3588	$-0.951 \pm j\,0.493, -17.582, -31.478$
	0.5	1.414	2.284	0.854	−0.3607	
	0.1	3.162	4.443	2.164	−0.2187	
0.5	1					
	0.5	1.000	2.068	0.800	−0.3046	
	0.4	1.118	2.261	0.906	−0.3006	$-0.95 \pm j\,0.157, -17.940, -32.382$
	0.3	1.291	2.544	1.069	−0.2081	
	0.1	2.236	4.111	2.887	−0.1287	

Table 2. Calculated estimator gain vectors and eigenvalues

Estimator No.	L_α	L_1	L_2	L_3	Eigenvalues	
1	L_A	0.6645	3.409	0.3549	−10	$-50 \pm j\,50$
2	L_B	0.9086	4.194	−4.396	−15	$-80 \pm j\,80$
3	L_C	0.7253	−0.8109	−0.7709	−15	$-25 -80$
4	L_D	0.9387	1.109	−2.554	−10	$-80 -100$
5	L_E	0.0879	2.448	0.1223	−10	$-25 \pm j\,25$
6	L_F	−0.1140	1.755	0.0189	−10	$-20 \pm j\,5$
7	L_G	−0.1140	1.954	0.0312	−10	$-20 \pm j\,10$
8	L_H	−0.1140	2.743	0.0796	−10	$-20 \pm j\,20$
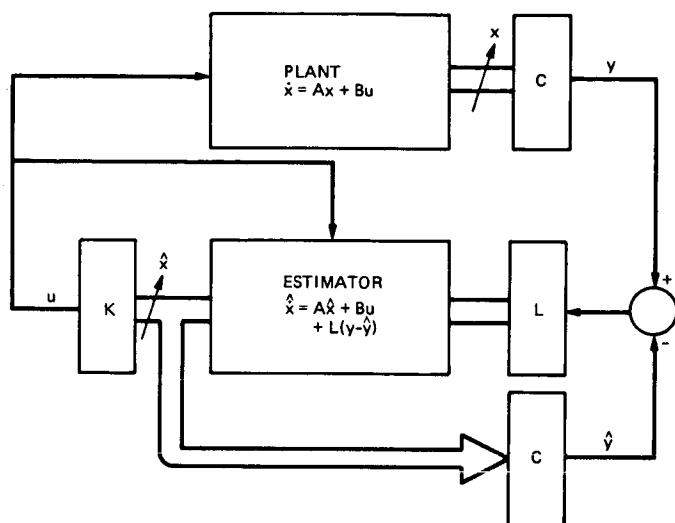
Fig. 1. State feedback with an estimator for a continuous time regulator
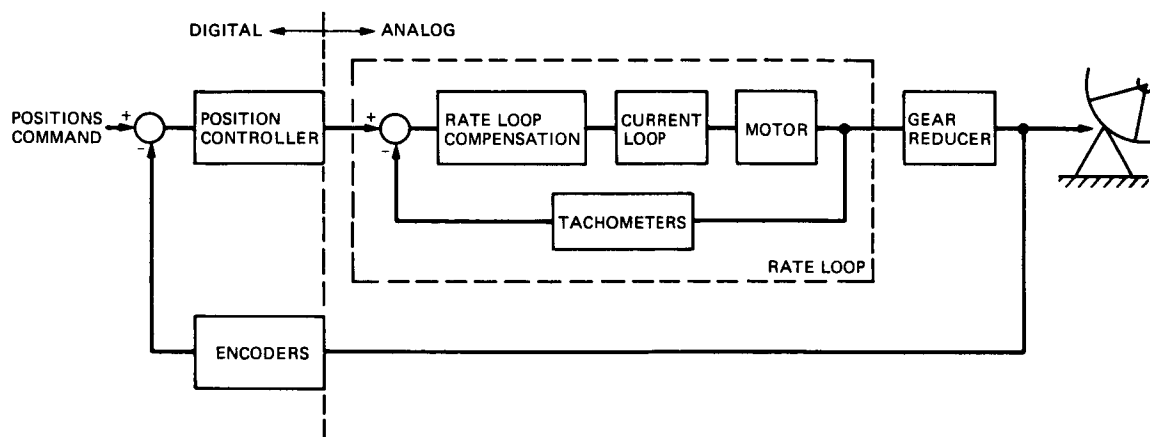
Fig. 2. Rate loop model
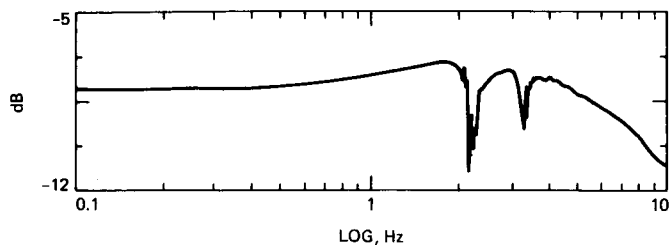
Fig. 3. DSS 15 elevation rate loop gain response
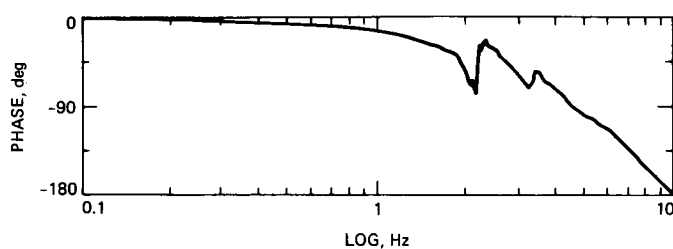
Fig. 4. DSS 15 elevation rate loop phase response
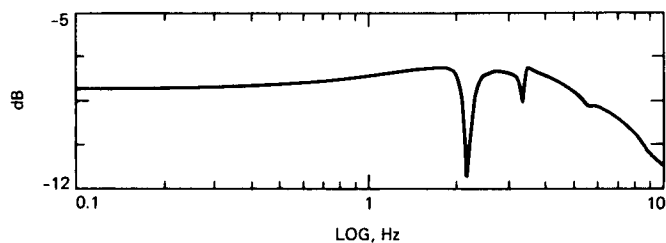
Fig. 5. Curve-fit gain response
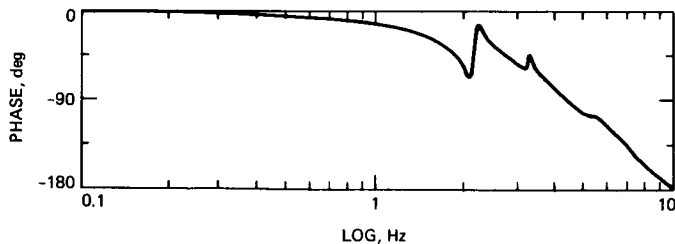
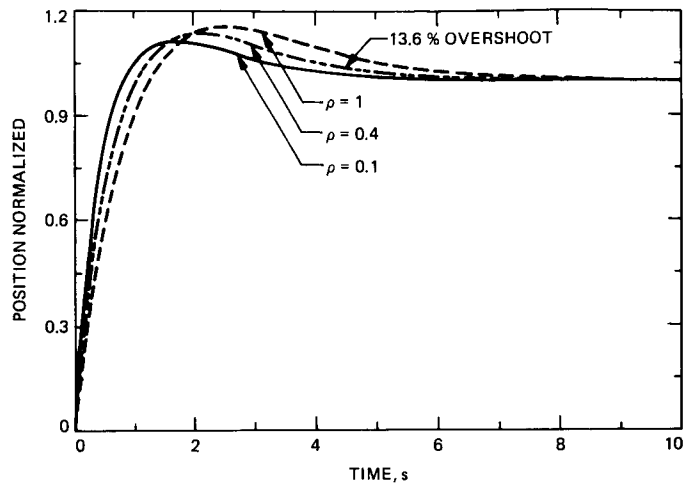**Fig. 6. Curve-fit phase response**

Fig. 7. Normalized step responses for Q = 0.5
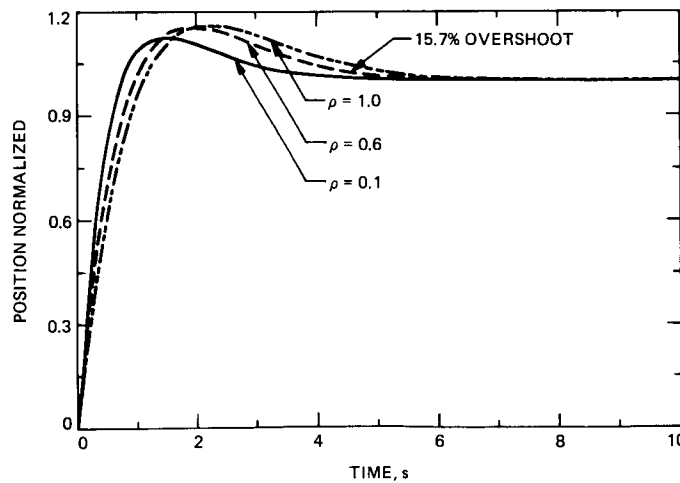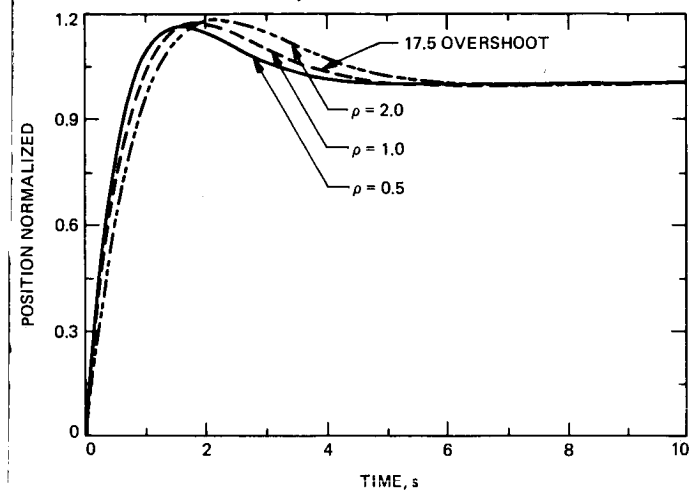

Fig. 8. Normalized step responses for Q = 1.0
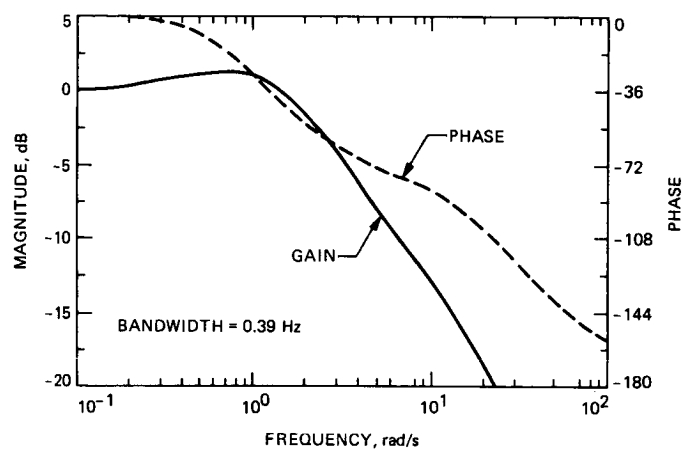
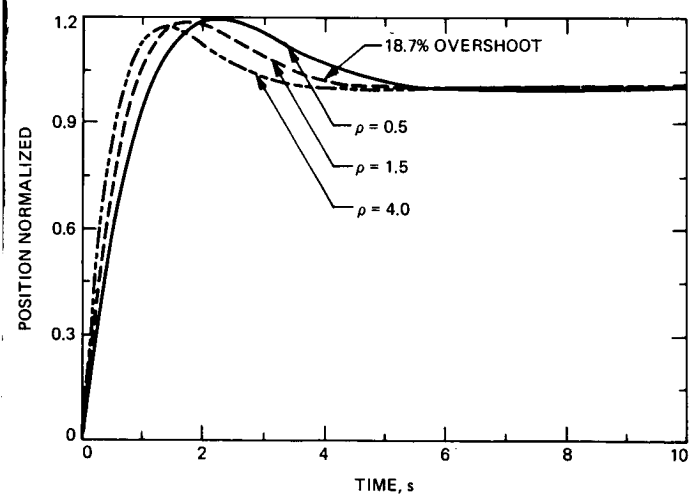Fig. 9. Normalized step responses for Q = 2.0

Fig. 11. Frequency response for Q = 0.5, ρ = 0.4

Fig. 10. Normalized step responses for Q = 4.0
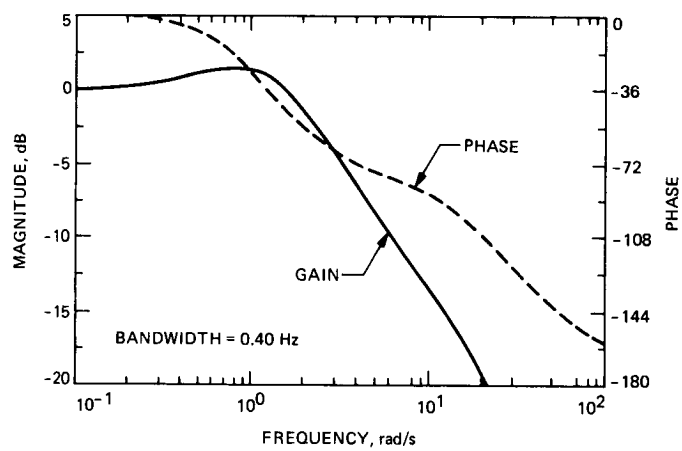
Fig. 12. Frequency response for Q = 1.0, ρ = 0.6
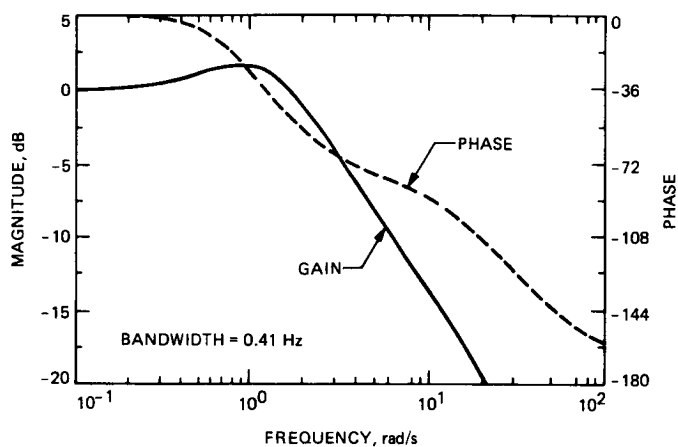
Fig. 13. Frequency response for Q = 2.0, ρ = 1.0
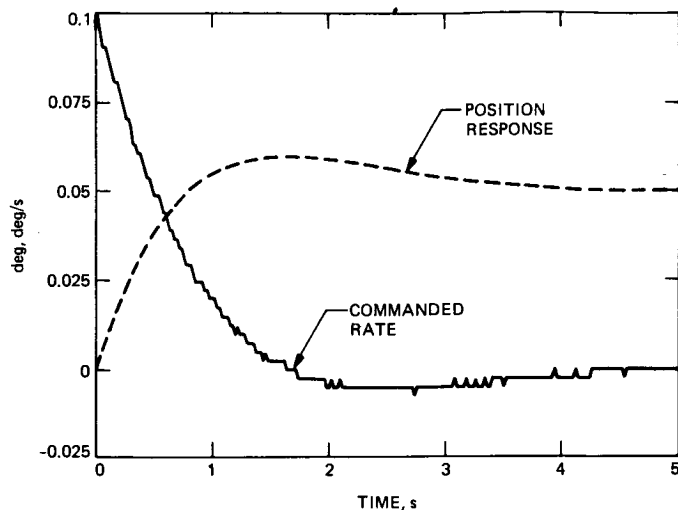
Fig. 15. Position and commanded rate responses for estimator 2
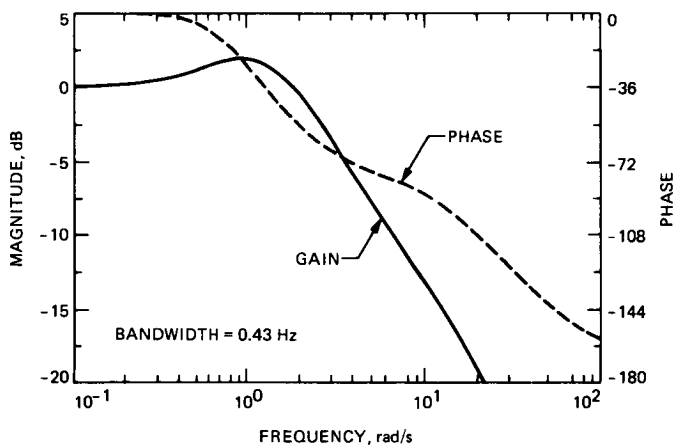
Fig. 14. Frequency response for Q = 4.0, ρ = 1.5
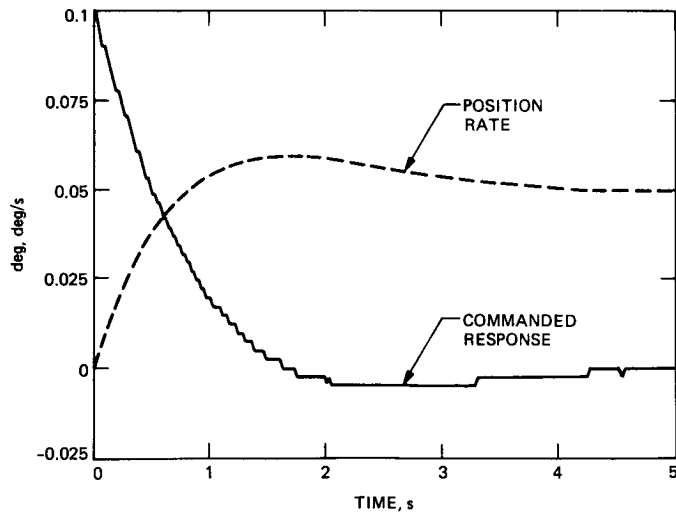
Fig. 16. Position and commanded rate responses for estimator 3
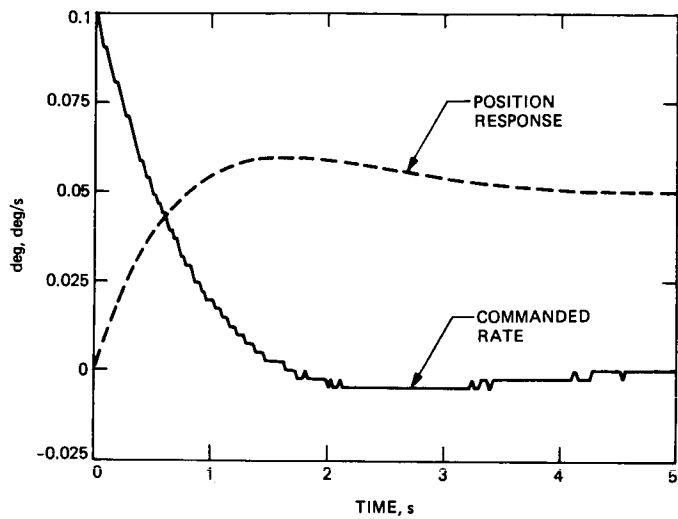
Fig. 17. Position and commanded rate responses for estimator 4
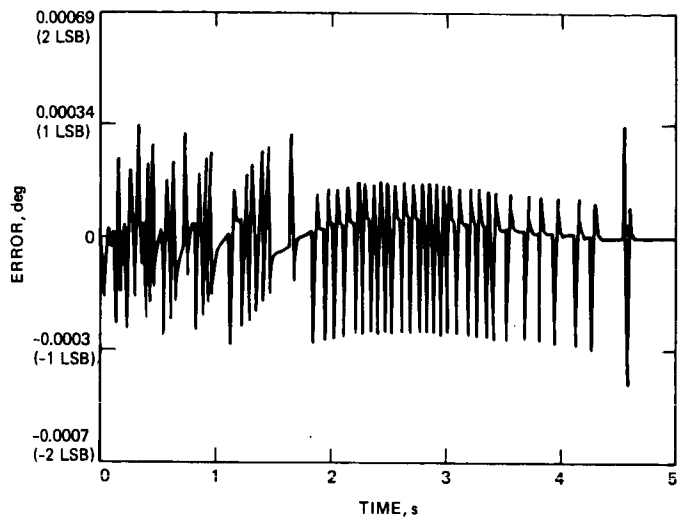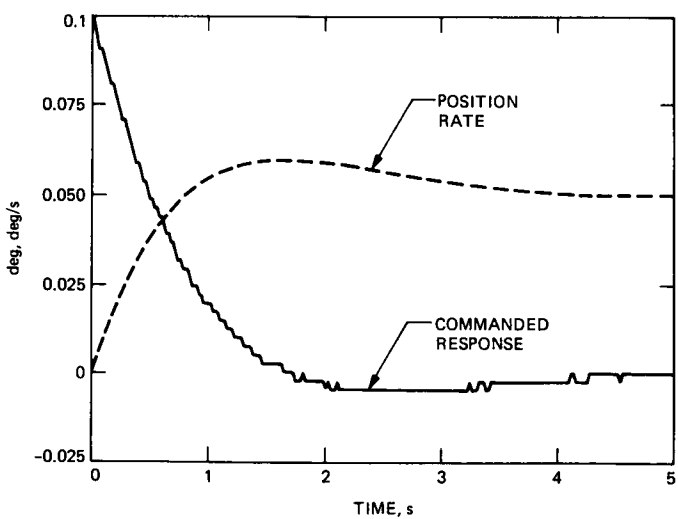

Fig. 19. Estimator 2's error response

Fig. 18. Position and commanded rate responses for estimator 7
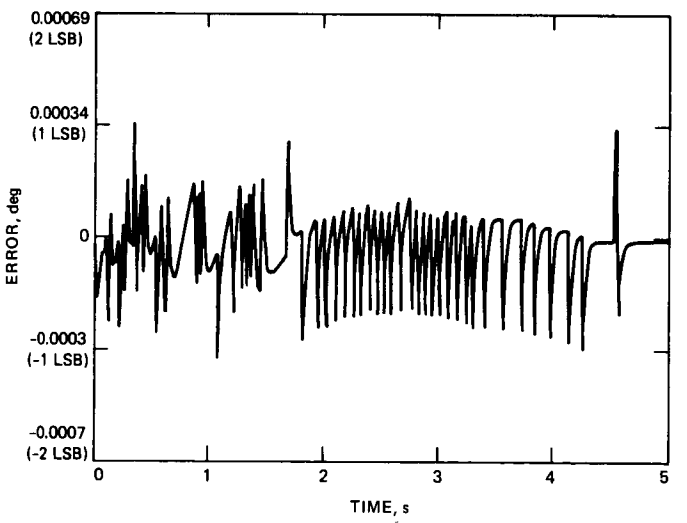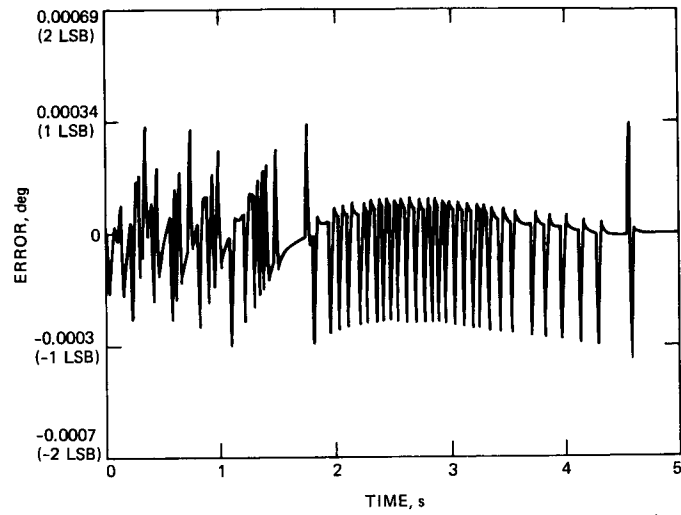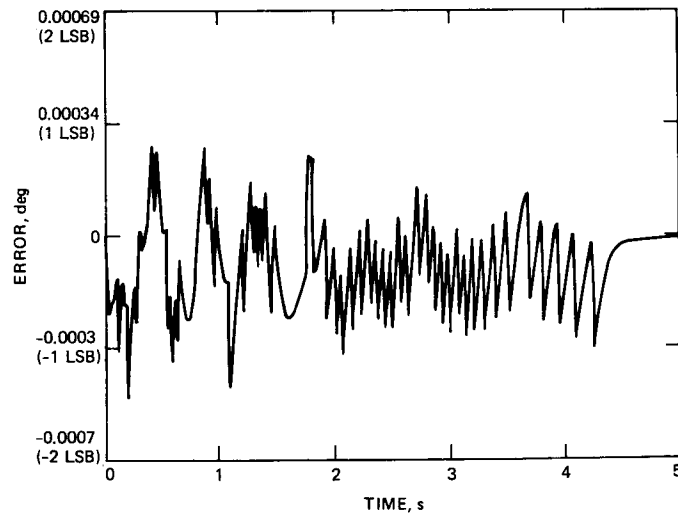

Fig. 20. Estimator 3's error response

Fig. 21. Estimator 4's error response

Fig. 22. Estimator 7's error response